ANALYSIS OF SPATIAL PLATE STRUCTURES

By

I. BOJTÁR

Department of Civil Engineering Mechanics, Technical University, Budapest

Received: October 18, 1978

Presented by Prof. Dr. S. KALISZKY

1. Introduction

The civil engineering practice is increasingly faced by the problem of the exact complex analysis of spatial structures. While earlier these problems have been reduced (both in numerical and in analytical handling) to plane problems (separately examining structural members), actually, the development of numerical methods and computers permits an integer analysis.

The most frequent problem is the analysis of structures consisting of plane members (e.g. panel buildings, swimming pools, reservoirs, some bridge types, etc.), advisably made by the finite element method.

Recent achievements in this scope at the Department of Civil Engineering Mechanics, Technical University, Budapest, will be described below. To our best knowledge, there have been published few programs on the spatial analysis, and none on the spatial plastic analysis at all. Fundamentals of the finite element method will here be assumed to be known, hence needless to repeat. In particular, forces and reactions in the superstructure have been analyzed, omitting supports. Otherwise the structure may be either rigidly or elastically supported, in this latter case any bedding model may be applied.

2. Linear analysis

2.1 *General*

It is relatively simpler and more practical to perform the analysis on a structure of a material supposed to be ideal elastic, homogeneous and isotropic.

Since the structure consists of plane members, the finite element method (the computer program itself) is increased beyond the usual plane problem only inasmuch as — assuming the classic method of displacements for the compilation — the global rigidity matrix of the structure (rigidity of the *spatial* node) is composed of rigidities of the elementary *plane* nodes. A further simplification is to assume the members to lie exclusively in orthogonal planes.

In this case the role of transforming matrices ends, from the elementary (local) system, uninhibited passage to global co-ordinates is possible, of course respecting sign conventions. Otherwise, most of practically important problems are those of such orthogonal systems.

Applicability of the program much depends on the characteristics of the applied type of members, primarily, on the freedom degrees of the elementary node. Applying e.g. flexural plate units (with 3 degrees of freedom,

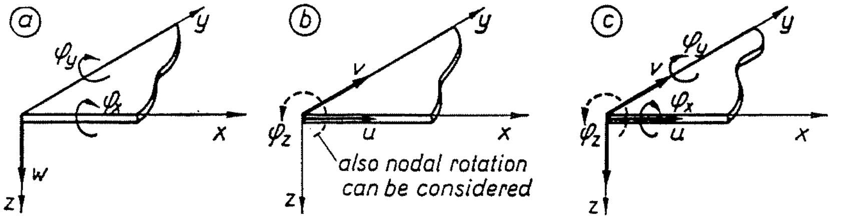

Fig. 1

two rotations and a displacement for each node, Fig. 1a), the structure itself is only subject to the membrane effect. In principle, the same is true for plane plates (Fig. 1b) where also spatial structures are markedly membrane-like. The first model lends itself for swimming pools, the second one for precast r.c. panel buildings. Obviously, it is the best to apply a type of member featuring both, i.e., to apply "plane shell units" (Fig. 1c).

By the way, even if the structural character is predominated by a given effect, it is advisable to use the latter general variety in the program, anyhow increasing the accuracy of the field of nodal displacements to be computed. The needless terms may be omitted at most in computing the stress components. Otherwise, the size (and running time) of the program is little reduced by applying the special variety, the number of degrees of freedom of the spatial node remaining six, and so the size of the global rigidity matrix does not change. Besides, it has to be cared that structural loads correspond to those of the model (e.g. in membrane structure no force normal to the member may be at a node where there is no member of force direction etc.). These statements have been confirmed numerically.

No stipulations on the member form are needed, since obviously, the above are unambiguously true for triangles, quadrangles, or even isoparametric general quadrangles.

2.2 *Refinement of linear models by the substructure method*

Obviously, engineering concepts are confined by computer capacities. The best way to accuracy is to densify the elements, resulting, however, in huge structural matrices. Even for computers with very large-capacity, theoretically sufficient storage units, running time would increase next to prohibitive.

To achieve a solution, either element properties have to be improved or/and construction of structural rigidity matrices modified by applying the method of substructures.

Its essential is to handle a given set of elements as an independent element of higher level, and to construct the global rigidity matrix from rigidity matrices of these "substructures". The substructure may be built up at two, essentially different levels. In the simpler solution, the boundary nodes remain global nodes. The complexer but also more efficient method, radically reducing the size of the global rigidity matrix, adds only some preferential nodes to the others, and specifies constraints for them (Fig. 2).

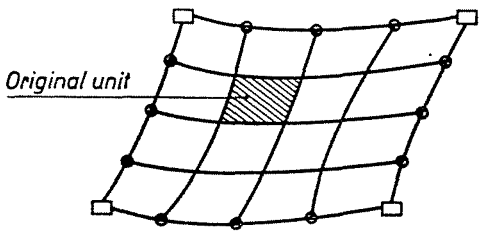

Fig. 2. □ node joining other substructures, ○ node under constraint

The above are independent of the member shape (triangle, quadrangle, etc.), type (plate diaphragm) or of its plane or spatial character. Obviously, composing simple plane members (keeping orthogonality) into some spatial structure, rigidity matrix of its substructures can unambiguously be given (Fig. 3).

Otherwise, this method facilitates consideration of openings in structural members at arbitrary places (e.g. windows in wall slabs).

Matrix equation

$$F = \mathbf{K} \cdot e \tag{1}$$

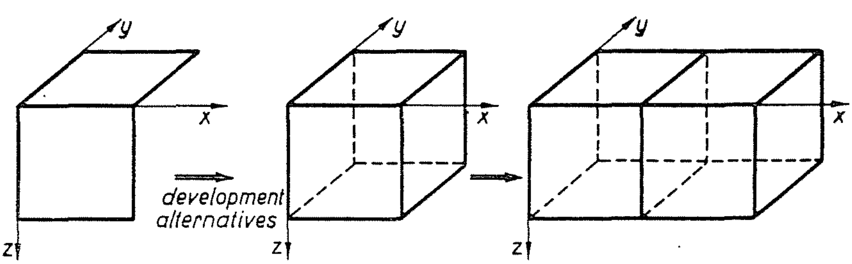

Fig. 3

relating nodal displacements e and nodal forces F of the set of members in Fig. 4 can be partitioned according to e.g. the second method such as:

$$\begin{bmatrix} 0 \\ F_e \\ F_c \end{bmatrix} = \begin{bmatrix} \mathbf{K}_{dd} & \mathbf{K}_{de} & \mathbf{K}_{dc} \\ \mathbf{K}_{ed} & \mathbf{K}_{ee} & \mathbf{K}_{ec} \\ \mathbf{K}_{cd} & \mathbf{K}_{ce} & \mathbf{K}_{cc} \end{bmatrix} \begin{bmatrix} e_d \\ e_e \\ e_c \end{bmatrix} \tag{2}$$

subscript d indicating the set of inner nodes, e the boundary nodes under special constraints, and c the global nodes joining adjacent elements. A basic stipulation is not to have outer forces at inner nodes, hence $F_d = 0$.

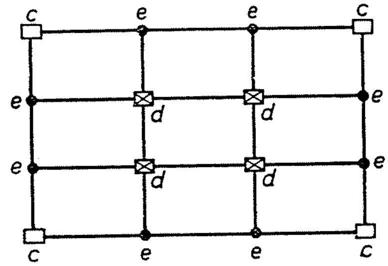

Fig. 4. □ node joining another member, ○ boundary node under constraint, ☒ inner node

Introducing constraint

$$e_e = \mathbf{G}_{ec} \cdot e_c \tag{3}$$

where $\mathbf{G}_{ec}$ is a matrix including special boundary conditions, e_d becomes:

$$e_d = \underbrace{-\mathbf{K}_{dd}^{-1}(\mathbf{K}_{de} \cdot \mathbf{G}_{ec} + \mathbf{K}_{dc})}_{\mathbf{A}} e_e \tag{4/a}$$

$$e_d = \mathbf{A} \cdot e_c \, . \tag{4/b}$$

Applying it for Eq. (2):

$$\begin{bmatrix} \mathbf{0} \\ \mathbf{F}_e \\ \mathbf{F}_c \end{bmatrix} = \begin{bmatrix} \mathbf{K}_{dd} & \mathbf{K}_{de} & \mathbf{K}_{dc} \\ \mathbf{K}_{ed} & \mathbf{K}_{ee} & \mathbf{K}_{ec} \\ \mathbf{K}_{cd} & \mathbf{K}_{ce} & \mathbf{K}_{cc} \end{bmatrix} \begin{bmatrix} \mathbf{A} \\ \mathbf{G}_{ec} \\ \mathbf{I} \end{bmatrix} e_c \, . \tag{5}$$

Properly transforming yields:

$$\mathbf{G}_{ec}^{*}\mathbf{F}_e + \mathbf{F}_c = \{\mathbf{A}^{*}(\mathbf{K}_{dd}\mathbf{A} + \mathbf{K}_{de}\mathbf{G}_{ec} + \mathbf{K}_{dc}) + \mathbf{G}_{ec}^{*}(\mathbf{K}_{ed}\mathbf{A} + \mathbf{K}_{ec} + \mathbf{K}_{ee}\mathbf{G}_{ec}) +$$

$$+ \mathbf{K}_{cd}\mathbf{A} + \mathbf{K}_{ce}\mathbf{G}_{ec} + \mathbf{K}_{cc}\} e_c \, . \tag{6}$$

Introducing notation $\mathbf{F}^* = \mathbf{G}^*_{ec}\mathbf{F}_e + \mathbf{F}_c$ and denoting the matrix in figure brackets by $\bar{\mathbf{K}}$:

$$\mathbf{F}^* = \bar{\mathbf{K}}\mathbf{e}_c \tag{7}$$

where $\bar{\mathbf{K}}$ is a substructure rigidity matrix to be used in the following. Utility of this method much depends on the efficient construction of matrix $\mathbf{G}_{ec}$.

Step-wise application of this method permits to decompose any spatial structure to substructures (even at several levels). Upon solution of the problem, inner node displacements needed for computing the stresses result from Eq. (2).

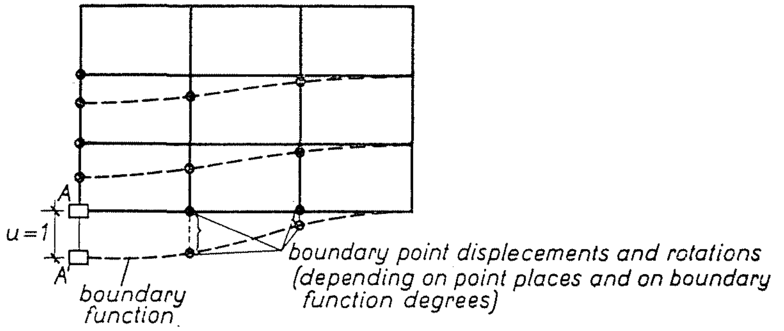

Fig. 5

In our computations, elements of matrix $\mathbf{G}_{ec}$ have been constructed by means of quadratic functions. Fig. 5 clearly shows how to determine from e.g. the unit displacement of global node A the displacement and rotation components of fixed boundary points.

It has been numerically observed that in simple panel structures needing about 1200 nodes for a practical solution, a tenth may be sufficient, decreasing the running time by two or three orders of magnitude.

3. Non-linear analysis

In the field of theoretical and experimental research, also for spatial structures, a means of development is to examine material and geometrical nonlinearities.

In this part, research on the analysis of the material nonlinearity of ordinary reinforced concrete plate structures will be reported on. Exclusively orthogonal structural systems have been examined, in fact, analyzed planewise. The effect of temperature, permanent or cyclic loads have been excluded, the structural members are considered as isotropic and homogeneous, at least by layer. Before going into details of practical computation steps, theoretical relationships underlying the program will shortly be recapitulated.

3.1 *Plasticity, cracking and ultimate condition*

3.11 *Concrete characteristics*

The examined structure is essentially in a plane stress state. Recently, research has been made throughout the world to determine relationships best fitting the concrete behaviour in these conditions. The most convincing test series have been made by KÜPFER, HILSDORF and RÜSCH [1] by the late

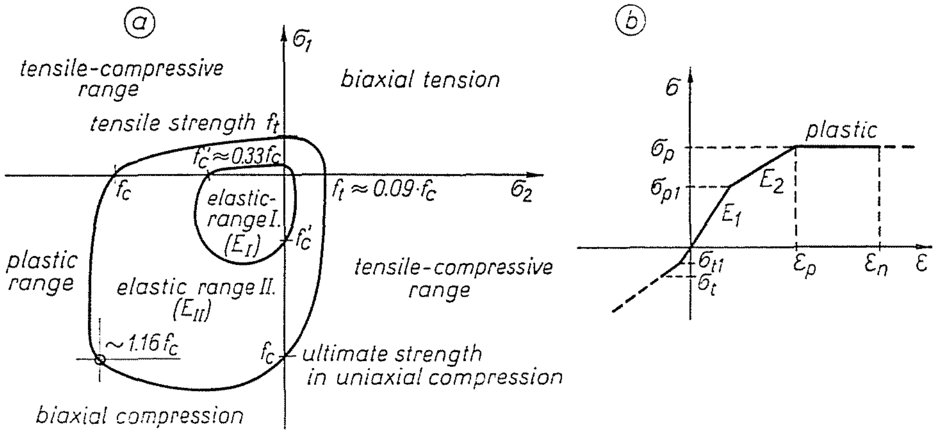

Fig. 6

'60s, our work relies on. Accordingly, concrete deformability may be bilinear elastic, rigid to tension and limited plastic to compression, then the concrete crumbles. Fig. 6 shows the ultimate condition curve of the concrete in biaxial stress state (as a function of principal stresses). As an illustration, it has been juxtaposed by the corresponding diagram of concrete in uniaxial stress state. The elastic range is seen to be divided into two parts of different moduli of elasticity.

In biaxial compression (both principal stresses being negative), the function describing the limit between elastic and plastic ranges may have different forms but most varieties refer essentially to the relationship between the octahedral shearing stress τ_{oct} and the hydrostatic stress p_{hyd}:

$$\tau_{\text{oct}} = a - b \cdot p_{hyd} \tag{8}$$

a and b being material constants.

From computation aspects, the function easiest to handle is that by *Huber—Mises—Hencky*:

$$\sigma_1^2 - \sigma_1 \sigma_2 + \sigma_2^2 = f_c^2 \tag{9}$$

where f_c is the uniaxial plasticity limit, σ_1, σ_2 being the principal stresses. This function is much exacter than the linear function applied by NIELSEN [2] and easier to program than those by CHEN [3] and SCHNOBRICH [4], at a difference of a few per cent. In ranges where at least one principal stress is

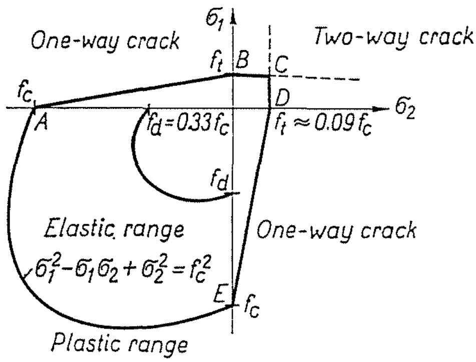

Fig. 7

tension, the cracking condition has been plotted in straight line in the numerical solution of the problem, see line $\overline{ABCDE}$ in Fig. 7. Characteristic points of straight sections may be expressed vs. the uniaxial compressive strength

The function describing the limit of the two elastic ranges is the same as (9) except for f_d rather than f_c in the right-hand side. As a failure condition, on the already plastic concrete an ultimate deformation was imposed where the material has perfectly lost its load capacity. This ultimate deformation is (see Fig. 8):

$$\varepsilon_1^2 - \varepsilon_1 \varepsilon_2 + \varepsilon_2^2 = \varepsilon_n^2 \tag{10}$$

where ε_n is the specific ultimate deformation. Of course, this function is only valid for negative principal strains.

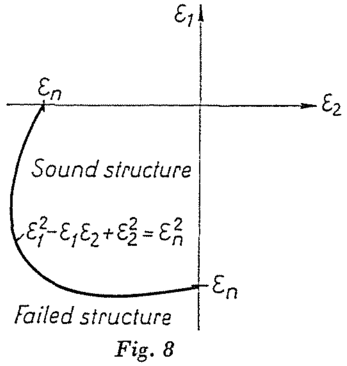

Fig. 8

3.12 *Reinforcement characteristics*

Reinforcement is supposed to be in uniaxial stress state. Applying a corresponding linear elastic—perfectly plastic material model, its behaviour is simple to follow (Fig. 9).

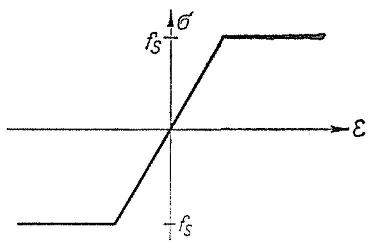

Fig. 9

3.2 *Stress-strain relationships*

Relationships between stress and displacement fields of elastic concrete and steel are readily available in the special literature [5], [6], not to be discussed here. Let us consider special cases:

a) *One-way cracked concrete*

In this case, a single principal stress in concrete attained the crack limit $\overline{\mathrm{ABCDE}}$ (Fig. 7). In the following, the tensorial notation, more common in the theory of plasticity, will be applied. Be σ_{ij} and ε_{ij} tensors of stresses and of specific deformations, resp., linearly related by tensor $\mathbf{C}_{ijkl}$. Now:

$$\sigma_{ij} = \mathbf{C}_{ijkl}\,\varepsilon_{ij} \tag{11}$$

where $\mathbf{C}_{ijkl}$ will be produced by the co-ordinate transformation of tensor $\overline{\mathbf{C}}_{ijkl}$, and

$$\mathbf{C}_{ijkl} = \begin{bmatrix} \mathrm{E} & 0 & 0 \\ 0 & 0 & 0 \\ 0 & 0 & \dfrac{\beta E}{2(1+\nu)} \end{bmatrix}.$$

The transforming matrix has to reckon with the deviation of the crack from the given direction, β being the shear capacity of the cracked concrete (about 0.4 according to tests).

b) *Two-way cracked concrete*

Both principal concrete stresses are at ultimate tension. Now:

$$\mathbf{C}_{ijkl} = 0.$$

c) *Plastic concrete*

For plastic concrete no relationship can be written between the total deformation and stress field, but increments can be related as:

$$\mathrm{d}\sigma_{ij} = \mathbf{A}_{ijkl}\,\mathrm{d}\varepsilon_k. \tag{12}$$

Let us determine tensor $\mathbf{A}_{ijkl}$ from considerations: deformation increments can be decomposed into two parts:

$$\mathrm{d}\varepsilon = \mathrm{d}\varepsilon^e + \mathrm{d}\varepsilon^p \tag{13}$$

$\mathrm{d}\varepsilon^e$ and $\mathrm{d}\varepsilon^p$ being elastic and plastic deformation increments, respectively. The elastic stress increment can be expressed as:

$$\mathrm{d}\sigma_{ij} = \mathbf{C}_{ijkl} \cdot \mathrm{d}\varepsilon_k^e \tag{14}$$

where $\mathbf{C}_{ijkl}$ is a known tensor. Substituting (13) into (14):

$$\mathrm{d}\sigma_{ij} = \mathbf{C}_{ijkl}(\mathrm{d}\varepsilon_k - \mathrm{d}\varepsilon_k^p). \tag{15}$$

According to the law of yield:

$$\mathrm{d}\varepsilon_k^p = \mathrm{d}\lambda\,\frac{\partial_f}{\partial\sigma_{kl}} \tag{16}$$

$\mathrm{d}\lambda \geqq 0$ being a place and time-dependent factor, and $f = f(\sigma_{ij})$ the yield function. Applying them, from (15):

$$\mathrm{d}\sigma_{ij} = \mathbf{C}_{ijkl}\left(\mathrm{d}\varepsilon_{kl} - \mathrm{d}\lambda\,\frac{\partial_f}{\partial\sigma_{kl}}\right). \tag{17}$$

Since in plastic condition $\mathrm{d}f = 0$:

$$\mathrm{d}f = \mathrm{d}\lambda \cdot \frac{\partial_f}{\partial\sigma_{ij}}\,\mathrm{d}\sigma_{ij} = 0\,. \tag{18}$$

Applying it, Eq. (17) will be multiplied all along by $\mathrm{d}\lambda\,\dfrac{\partial_f}{\partial\sigma_{ij}}$:

$d\lambda$ can be factored out. Resubstituting into (17) yields the fundamental relationship:

$$d\sigma_{ij} = \left[\mathbf{C}_{ijkl} - \frac{C_{ijrs} \dfrac{\partial f}{\partial \sigma_{rs}} \cdot C_{pqkl} \dfrac{\partial f}{\partial \sigma_{pq}}}{C_{pqrs} \dfrac{\partial f}{\partial \sigma_{pq}} \cdot \dfrac{\partial f}{\partial \sigma_{rs}}} \right] d\varepsilon_{kl} \tag{20}$$

the term in brackets being the tensor $\mathbf{A}_{ijkl}$ sought for.

Of course, it simplifies in the bidimensional case into:

$$\mathbf{B}_{pqrs} = \mathbf{A}_{pqrs} - \frac{\mathbf{A}_{pq33} \cdot \mathbf{A}_{33rs}}{\mathbf{A}_{3333}} \tag{21}$$

and

$$d\sigma_{pq} = \mathbf{B}_{pqrs} \cdot d\varepsilon_{rs}$$

to be used in the following.

d) *Crumbled concrete*

Load capacity of concrete in the plastic range is suppressed at the ultimate deformation. Beyond the limit in (10), the tested unit fails, hence:

$$\mathbf{C}_{ijkl} = 0\,.$$

e) *Plastic reinforcement*

In the plastic range, the reinforcement cannot bear more load, hence also here:

$$d\sigma_{ij} = 0\,.$$

3.3 *Modification of material characteristics*

Modification of material characteristics is accompanied by stress excesses:

$$\Delta\sigma = \sigma_0 = \sigma_n \tag{23}$$

where $\Delta\sigma$ is the excess, σ_0 and σ_n are stresses calculated with previous and actual material characteristics, respectively.

In analysis, most difficulties arise in determining $\Delta\sigma$ for plastic concrete. There are two basic cases:

3.31 *Elastic concrete turned plastic*

In course of loading (Fig. 10), initial value σ_0 turns $\bar{\sigma}$ with the previous material characteristics. This stress change causes a strain $d\varepsilon$, of which $d\varepsilon^p$ is plastic strain (passing to the plastic range at σ^p). Using σ^p and ε^p, by means of matrix $\mathbf{B}_{ijkl}$ $\bar{\sigma}^p$ is obtained. Adding it to σ^p yields σ^*, its projection onto the failure surface yields σ^{p*} hence:

$$\Delta\boldsymbol{\sigma} = \bar{\boldsymbol{\sigma}} - \boldsymbol{\sigma}^{p*} \tag{24}$$

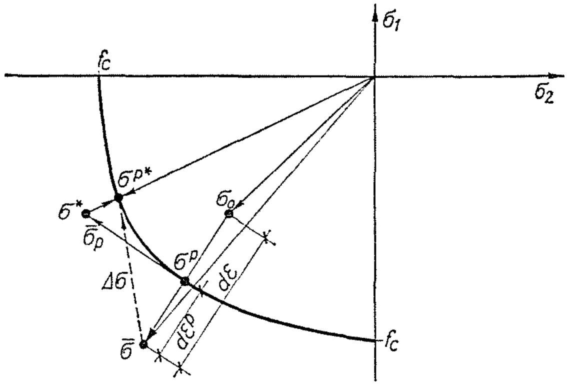

Fig. 10

3.32 *Plastic concrete remains plastic* (*Fig. 11*)

The previous stress state is σ_0, pertaining material characteristics being included in $\mathbf{B}$. Upon a plastic deformation increment $d\varepsilon^p$:

$$\boldsymbol{\sigma}^* = \boldsymbol{\sigma}_0 + \bar{\boldsymbol{\sigma}}^p = \boldsymbol{\sigma}_0 + \mathbf{B}d\varepsilon \tag{28}$$

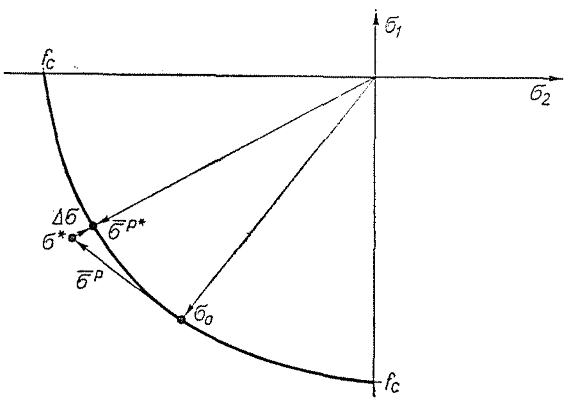

Fig. 11

B being the plastic stress-strain matrix. Projecting the resulting stress tensor onto the failure surface yields:

$$\Delta\boldsymbol{\sigma} = \boldsymbol{\sigma}^* - \boldsymbol{\sigma}^{p*}.$$

3.4 *Main steps of analysis*

For the practical implication of the above on spatial structures, a computer program has been made. A composite plane quadrangular member — reckoning with both plate and diaphragm effect — is applied, where all partial members are multilayered (Fig. 12). Construction of the elementary rigidity

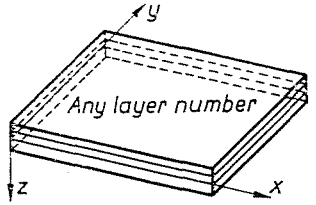

Fig. 12

matrix is somewhat different from the conventional explicit one because of the stratification, namely now integration along the thickness can only be performed from layer to layer. Main steps of the analysis are:

1. Nodal displacements are determined from the effect of the expediently chosen force increments in the structure. Thereafter plane by plane, the following set of steps will be performed on each member:
   1,1 From nodal displacements, median surface deformations are computed and each layer of that member will be subjected to the following:
      1,1,1 Layer deformations are computed from median surface values.
      1,1,2 Applying previous material characteristics, layer stresses are computed, either in the member centre, or, advisably, using so-called integrated mean stresses.
      1,1,3 This stress state will be compared to the given boundary conditions. If none has been transgressed, item 1,1,6 may follow.
      1,1,4 Computing increments between stresses, they are added to the stress increment vector of the member.
      1,1,5 If the rigidity matrix has to be changed, then the corresponding matrix **C** of the member will be modified by using the difference between the old and the new material characteristics.
      1,1,6 If there are several layers, set of steps 1,1,1 to 1,1,5 will be iterated.

1,2 If none of the change conditions are met in the member, item 3 will be passed on. Else, nodal forces from stress increments are computed and stored in a global force increment vector.

1,3 If needed, rigidity matrix of the structures is modified. The classic principle that, when the structural rigidity matrix is modified, only the elementary rigidity matrix constructed from the difference between new and old material characteristics has to be deduced from the original global rigidity matrix, can only be applied on large computers and for small problems.

2. For still unchecked members, steps (1,1 to 1,3) have to be repeated, otherwise the structure is re-examined for force increment vector effects.
3. Displacements are checked for convergency. In the positive case, computation is repeated from 1. If the analysis diverges or the permitted number of iterations has been passed, the program stops.

4. Remark

The program family developed on the basis of the presented methods lends itself for the linear or bilinear-elastic—limited plastic analysis of arbitrarily supported, orthogonally positioned spatial plate structures (with diaphragm or plate features). The programs have been tested on different problems, yielding practically adequate results. A further problem will be theoretical and practical development of the non-linear elastic—plastic analysis.

Summary

In recent years, numerical analysis of spatial structures has been made at the Department of Civil Engineering Mechanics. Achievements with linear models are described, together with improvement possibilities. A special chapter is spent on computation methods applicable for structures accessible to non-linear elastic-plastic material models of limited deformability.

References

1. Küpfer, H.–Hilsdorf, H.K.–Rüsch H.: Behavior of Concrete under Biaxial Stresses. ACI Journal, August 1969.
2. Nielsen: On the Strength of Reinforced Concrete Discs. A.P.S. Copenhagen 1971.
3. Chen, W. F.: Limit Analysis. McGraw Hill, New York 1975.
4. Schnobrich, W.: A Layered F.E.M. Analysis of Reinforced Concrete Plates and Shells. Civil Eng. Studies, Illinois 1972.
5. Kaliszky, S.: Theory of Plasticity.* Akadémiai Kiadó, Budapest 1975.
6. Bezukhov: Introduction into the Theory of Elasticity and Plasticity.* Tankönyvkiadó, Budapest, 1952.

* In Hungarian.

Imre Bojtár, H-1521, Budapest